

Fission of targetlike fragments populated in the multinucleon transfer reactions of 340 MeV ^{28}Si on ^{232}Th

A. Saxena,¹ D. Fabris,² G. Prete,³ D. V. Shetty,³ G. Viesti,² B. K. Nayak,¹ D. C. Biswas,¹ R. K. Choudhury,^{1,6}
S. S. Kapoor,¹ M. Barbui,³ E. Fioretto,³ M. Cinausero,³ M. Lunardon,² S. Moretto,² G. Nebbia,² S. Pesente,² A. M. Samant,²
A. Brondi,⁴ G. La Rana,⁴ R. Moro,⁴ E. Vardaci,⁴ A. Ordine,⁴ N. Gelli,⁵ and F. Lucarelli⁵

¹*Nuclear Physics Division, Bhabha Atomic Research Centre, Mumbai 400 085, India*

²*Dipartimento di Fisica and Sezione INFN Padova, I-35131 Padova, Italy*

³*INFN Laboratori Nazionali di Legnaro, I-35020 Legnaro (Pd), Italy*

⁴*Dipartimento di Scienze Fisiche and Sezione INFN Napoli, I-80126 Napoli, Italy*

⁵*Dipartimento di Fisica and Sezione INFN Firenze, I-50125 Firenze, Italy*

⁶*Institute of Physics, Bhubaneswar 751 005, India*

(Received 27 November 2001; published 22 May 2002)

The transfer-induced fission channel has been studied in the collision of 340 MeV ^{28}Si on ^{232}Th as a function of the atomic number of the projectilelike fragments (PLF's) by using a 4π detector array. It is found that the energy loss of the transfer reaction increases as a function of the net charge transfer ΔZ from the projectile to the target nucleus, going from quasielastic to deep-inelastic regimes. The average excitation energy of the targetlike fragment (TLF) is derived from the measured energy loss, whereas its angular momentum has been obtained from the angular distribution of fission fragments. It is found that the populated TLF nuclei with $Z_{TLF}=90-96$ ($\Delta Z=0-6$) have average excitation energies up to about 100 MeV and angular momenta up to about $40\hbar$. The measured ratio of transfer-fission yield to PLF singles, Y_f , first increases with increasing net charge transfer up to $\Delta Z=4$ and then shows a plateau around the values $Y_f=0.4-0.6$ followed by a decrease for higher ΔZ transfers. This ratio can be identified as the cumulative fission probability of the populated nuclei for net charge transfers up to $\Delta Z\leq 6$, where a two-body mechanism for the first reaction step is supported by the experimental data. This result suggests a significant survival probability against fission of these TLF nuclei, in marked disagreement with the standard statistical model predictions. The observed survival probability implies that there is a strong hindrance to fission in the early stages of deexcitation, as also indicated by the large fission times ($t_f=10-100$ zs) derived from earlier neutron measurements in fusion-fission reactions. The importance of such effects in the population of nuclei in the heavy and superheavy mass regions by transfer reactions is discussed.

DOI: 10.1103/PhysRevC.65.064601

PACS number(s): 25.70.Jj

I. INTRODUCTION

Transfer reactions on heavy targets offer the possibility to populate a wide range of targetlike fragment (TLF's) nuclei at varying excitation energies, which can be used to study in a systematic way the fission reaction mechanism. In particular, the study of the fission probability P_f of TLF nuclei is not only interesting by itself, for providing information on the fission dynamics [1], but also because it gives a direct measure of the probability of survival of the populated TLF nuclei, thus exploring the possibility to produce specific nuclear species by means of the transfer reactions [2].

It is now well established that the fission process is dominated by effects due to the nuclear viscosity, which produce a strong hindrance to fission. Extensive studies have been carried out in the past to obtain information on the fission dynamics and in particular to determine the fission time scales (t_{fiss}) from the measurements of prescission neutrons, protons, alpha particles, and electric dipole γ rays, in fusion-fission reactions [3-7]. All these studies gave a strong indication of the dynamical delay in the fission process, although the derived fission times are somewhat dependent on the statistical model parameters used in the analysis. Moreover, fission probabilities have also been directly measured in

transfer-induced fission reactions [8-10]. A comparison between the experimental fission probabilities and the statistical model predictions provides a direct way to study the fission dynamics under the condition that the mass, charge, excitation energy, and angular momentum of the fissioning TLF nuclei can be reliably derived from the experimental observables.

Fission probabilities of TLF nuclei populated in transfer reactions are of particular interest, when these nuclei lie in the mass region of very heavy and superheavy elements. Dynamical model studies for the synthesis of superheavy nuclei have shown that the fission hindrance factor can play a significant role in the survival probability against fission of the populated composite systems [11]. Therefore detailed knowledge of the fission dynamics as deduced from direct measures of the fission probability of very heavy nuclei should prove to be useful to establish the optimal conditions for the synthesis of these exotic nuclear species.

An experimental project has been started at the accelerator facility of the Laboratori Nazionali di Legnaro, with the aim to study the role of fission dynamics in transfer induced fission reactions, by using a newly completed 4π charged particle detector system. This experimental setup is designed for simultaneous detection of light charged particles and fis-

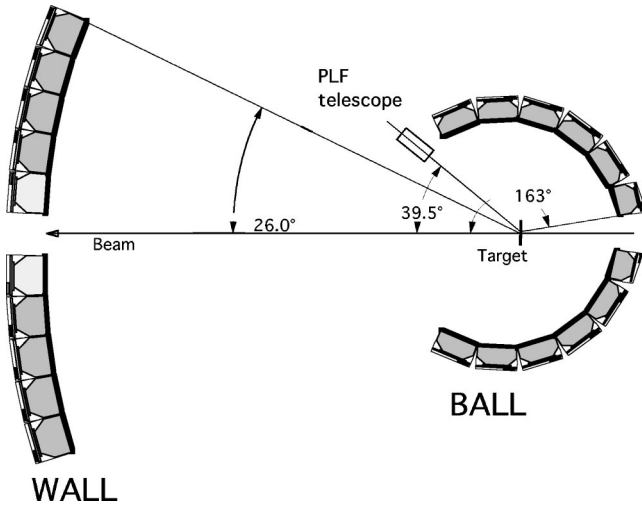


FIG. 1. Schematic layout of the experimental setup; for details, see text.

sion fragments using the same detector elements and offers the large detection efficiency needed in a detailed investigation of transfer-fission reactions. As a first step of this program, a study has been completed for the reaction of 340 MeV ^{28}Si on ^{232}Th . The results obtained in this work are presented in this paper.

II. EXPERIMENTAL DETAILS AND DATA ANALYSIS

The experiment has been performed at the XTU Tandem–ALPI Super-conducting LINAC accelerator complex of the Laboratori Nazionali di Legnaro. A 340 MeV ^{28}Si beam, of about 1 pA intensity was used to bombard a self-supporting ^{232}Th target of 1.5 mg/cm² thickness.

The 8π LP detector [12], shown schematically in Fig. 1, was employed. It consists of two detector subsystems made of ΔE - E telescopes: the WALL and the BALL. The WALL is placed at 60 cm from the target, covering angles from $\Theta_{lab} = \pm 10^\circ$ to $\Theta_{lab} = \pm 26^\circ$, where Θ_{lab} indicates the angle between each detector and the beam direction. The BALL has 15 cm internal radius, covering in this experiment angles from $\Theta_{lab} = \pm 51^\circ$ to $\Theta_{lab} = \pm 163^\circ$. Each telescope is made of a transmission 300- μm -thick Si detector followed by a CsI(Tl) crystal, 15 mm or 5 mm thick for the WALL and the BALL, respectively, to stop light charged particles with energies up to 64A MeV and 34A MeV. The WALL is a matrix of 11×11 telescopes, missing the four positioned at the corners, and the central ones to exit the beam. The WALL detectors are all identical in shape with an active area of 25 cm², which corresponds to an angular opening of $\Delta\Theta_{lab} = 4^\circ$. The BALL consists of six rings of 18 telescopes each with trapezoidal shapes and active areas ranging from 7.2 cm² to 17.8 cm², subtending solid angles from 32 msr to 79 msr. The majority of the BALL detectors have an angular opening of about $\Delta\Theta_{lab} = 17^\circ$.

The ΔE - E and time-of-flight techniques are used for particle identification in the WALL telescopes, with an energy threshold as low as 0.5A MeV. The same low-energy threshold characterizes the BALL telescopes, for which particle

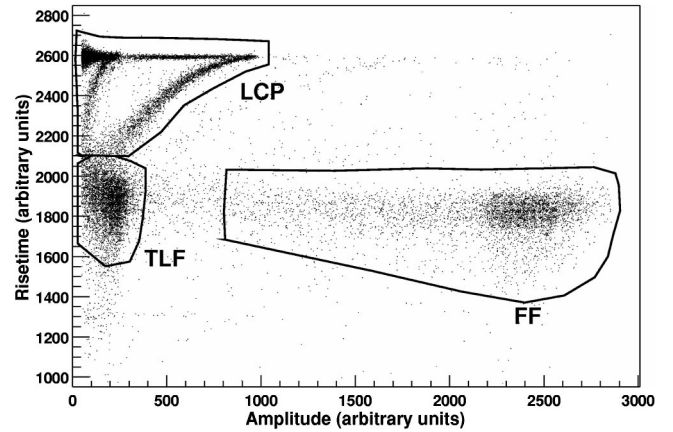


FIG. 2. Example of raw particle identification matrix (signal rise time versus amplitude) in a silicon detector of the BALL. FF, LCP, and TLF identify the regions where fission fragments, light charged particles, and targetlike fragments are located.

identification is obtained by using a combination of ΔE - E and pulse shape analysis techniques [13]. For this purpose, BALL-Si detectors are mounted in the “flipped” mode (with particles entering from the Ohmic side), so that the ions stopped in the Si can be identified looking at the correlation between risetime and amplitude of the signal. In this way light particles and fission fragments are well discriminated, as shown in Fig. 2.

As the grazing angle in the present experiment is about $\Theta_{lab} = 40^\circ$, a 200- μm -thick aluminum foil was placed in front of the WALL to avoid the radiation damage of the semiconductor detectors. The WALL detectors, therefore, could not be used as fission fragment detector. Projectilelike fragments (PLF’s) were detected using a ΔE - E telescope, made of 40 μm +400 μm thick silicon detectors, placed around the grazing angle ($\Theta_{lab} = 39.5^\circ$) with a solid angle coverage of 1.3 msr.

Remote, automatic control of all the electronic settings was performed by a LabView [14] based program which controls the constant fraction discrimination thresholds, the amplifier gains, the bias supply, and the leakage currents. Because of the flipped mounting, the response of each BALL silicon detector was particularly sensitive to its bias supply. An update of the bias values was periodically performed during the experiment, to ensure stable and correct depletion of all silicon detectors.

The data acquisition is based on the FAIR (fast inter-crate readout) bus system [15]. The FAIR bus is based on a hardware level protocol that allows event building and synchronous data transfer without the need of a dedicated CPU. During the data taking, the acquisition rate was $\approx 1.5 \times 10^3$ events per second with a dead time of 20% mainly due to the conversion time and the storage of the events on tape.

The trigger of the acquisition system was generated by the detection of a particle in the PLF detector or a twofold event in the BALL. WALL detectors were collected in slave mode.

For the off-line data analysis, specific classes were developed in C++ language and linked to the ROOT software package [16]. The geometry of the 8π LP detector was also

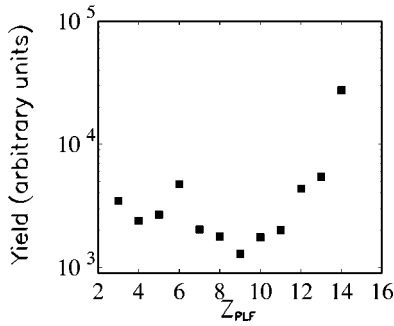


FIG. 3. Yield of the projectilelike fragments versus the fragment atomic number Z_{PLF} .

folded in the off-line software. The first step in the data analysis was to create an identification parameter for each type of detected particle (or fragment) to easily correlate PLF's, fission fragments, and light particles detected in any event. These parameters were added to the raw data and a new data set was created and used in the subsequent analysis.

III. EXPERIMENTAL RESULTS

A. Projectilelike fragment single results

Figure 3 shows the observed yield of the PLF nuclei versus the fragment atomic number, Z_{PLF} , as measured in single mode by silicon telescopes placed at grazing angles. It is expected that the relative yield of PLF's should decrease when the net charge transfer $\Delta Z = 14 - Z_{PLF}$ is increased. This trend, well evident in Fig. 3 for $Z_{PLF} > 9$, is a feature of the quasielastic transfer reactions, where the relevant parameter in determining the production rate is the Q value. On the other hand, in case of deep-inelastic collisions, the potential energy surface of the dinuclear system determines mainly the element distribution [17]. The first moment of the element distribution might move far from $Z = Z_{beam}$, depending on the driving force that governs the charge equilibration between PLF's and TLF's. The width of the distribution generally increases with the energy loss, being large for completely relaxed events. A broad distribution is also seen in Fig. 3 for $4 \leq Z_{PLF} \leq 9$. We note, however, that the production yield for $Z_{PLF} = 6$ appears to be enhanced with respect to the neighboring elements. The preferential production of this isotope cannot be explained by a simple collision mechanism. On the contrary, it can be due to an additional production mechanisms during (as projectile breakup) or after (as sequential PLF decay) the reaction [8]. This point will be further discussed in the following sections. Finally, the yields in Fig. 3 are dominated at $Z_{PLF} \leq 3$ by the evaporation processes.

The energy spectra of PLF nuclei were found to be of nearly Gaussian shape, with a width increasing with the net charge transfer ΔZ . The width is in the range of about 20–60 MeV for transfer channels up to $\Delta Z \leq 6$. The average energy loss $\langle EL \rangle$ deduced from the observed energy spectra of projectilelike fragments of different atomic number Z_{PLF} , detected in single mode, is shown in Fig. 4. For comparison, the calculated energy loss for the case of complete damping

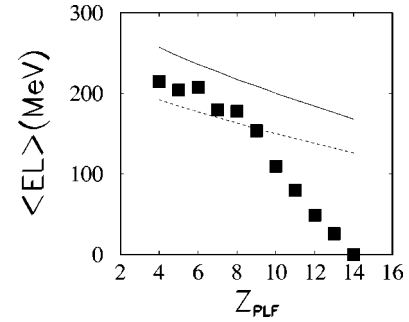


FIG. 4. Experimental average energy loss $\langle EL \rangle$ as a function of the projectilelike fragment Z_{PLF} (squares). The solid line refers to the calculated energy loss corresponding to the full relaxation of the kinetic energy. The dashed line correspond to about 75% of the full relaxation limit.

of kinetic energy, i.e., corresponding to the Coulomb energy in the exit channel between two touching spheres, is also reported in the figure. As commonly seen in two-body collisions around this bombarding energy, the energy loss increases with the net charge transfer ΔZ [17]. For low values of ΔZ , the inelasticity is quite low as in quasielastic collisions. For $\Delta Z > 5$ (i.e., $Z_{PLF} < 9$) the energy loss indicates a sizable dissipation, approaching about 80% of the full damping limit.

The measured energy loss can be used to infer the excitation energy of the reaction partners $E_x(\text{PLF})$ and $E_x(\text{TLF})$, once its sharing between PLF's and TLF's is evaluated. It is well known [9,18] that the energy sharing between the fragments evolves in a continuous way from the quasielastic regime, where the limit of equal excitation energy for PLF's and TLF's is well demonstrated, to the fully relaxed events, where the thermal equilibrium hypothesis is assumed for the excitation energy sharing. Furthermore, we note that typical spin values of (30–40) \hbar have been determined for heavy fragments populated in deep-inelastic collisions up to 140 MeV excitation energy [19].

The relevant parameters of the nuclei produced in the transfer reactions of ^{28}Si on ^{232}Th were extracted in the following way.

(1) The most probable mass for the PLF fragment, $\langle A_{PLF} \rangle$, has been obtained for each Z_{PLF} taking the minimum value of the ground-state Q value (Q_{gg}) corresponding to that transfer reaction. This choice defines the most probable mass and charge of the corresponding primary TLF fragments in the hypothesis of mass and charge conservation. This point will be further discussed in the Sec. III B 2.

(2) The average total excitation energy available to the fragments is then computed from the measured average energy loss $\langle EL \rangle$ and the Q_{gg} value.

(3) An empirical energy sharing function has been derived from experimental and theoretical predictions reported in Ref. [18] for the collisions of 8.5 MeV/nucleon ^{56}Fe on ^{238}U target. This function gives $E_x(\text{TLF}) = E_x(\text{PLF})$ for $EL = 0$, reaching roughly the 80% of the thermal equilibrium condition for $EL = 150$ MeV.

(4) The average spin transferred to the TLF fragments has been determined from the fission fragment angular distribu-

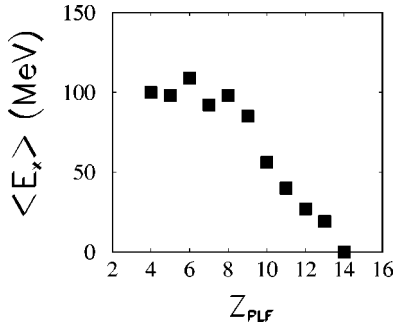


FIG. 5. Estimated average excitation energy $\langle E_x \rangle$ for TLF nuclei as a function of Z_{PLF} . For details see the text.

tions, as discussed in Sec. III B 1. These values have been checked to be consistent with those obtained in Ref. [19] for heavy deep-inelastic reaction products.

The average excitation energy values $\langle E_x \rangle$ of TLF fragments extracted as above are reported in Fig. 5. It may be pointed out that there is a spread in the excitation energy of the TLF fragments around these average values due to the width of the mass and energy loss distributions of PLF. Furthermore, the average excitation energy values might be affected by the assumptions made in defining the partition of energy between PLF and TLF nuclei. Both aspects are further discussed in Sec. IV with respect to fission probabilities evaluated within the statistical model.

B. Transfer-induced fission results

1. Fragment angular distributions

The fission fragment angular distributions with respect to the recoil axis of the fissioning system and, in particular, the fission fragment anisotropies [$W(0^\circ)/W(90^\circ)$] carry valuable information on the angular momentum in the fission channel and on the fission K_0^2 parameter, i.e., the variance of the K distribution of the fissioning system.

In the present experiment, the reaction plane is identified by the beam axis and by the PLF trigger detector position. For each detected PLF, the average recoil angle of the corresponding TLF is derived from the two-body kinematics using the measured average energy loss $\langle EL \rangle$. Consequently, the relative angle between the recoiling (undetected) TLF and each BALL detector is obtained.

As an example, Fig. 6 shows the observed fragment angular distribution relative to the derived TLF recoil angle in the case of $Z_{PLF} = 12$. The observed angular distributions were fitted with the function $A + B \cos^2 \theta$ to deduce the angular anisotropies for different Z_{PLF} , as reported in Fig. 7. It is seen that the anisotropy increases with increasing net charge transfer, as qualitatively expected from simple considerations of the angular momentum transferred to TLF's [17]. However, this trend shows a discontinuity around $Z_{PLF} = 9-10$. From the experimental point of view, the data reported in Fig. 7 can be compared with results from previous measurements. In particular, transfer-fission data on ^{232}Th target have been reported in Ref. [20]. In that case, the measured in-plane anisotropy for the near-barrier reaction

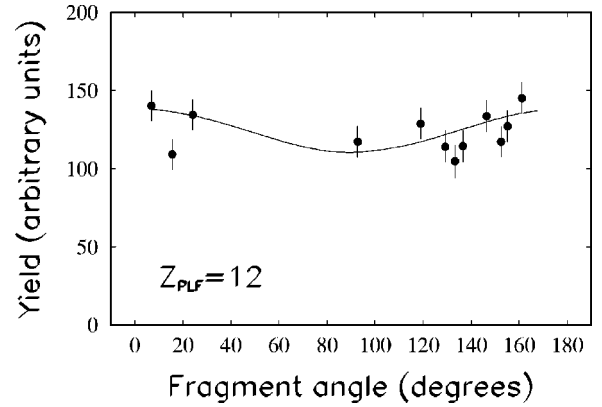


FIG. 6. Typical angular distribution of fission fragments measured in coincidence with projectilelike fragments having $Z_{PLF} = 12$. The fragment angle is relative to the derived TLF recoil direction. The line refers to a fit to the experimental data. For details see the text.

$^{232}\text{Th}(^{16}\text{O},\text{C})$ was found to be $W(0^\circ)/W(90^\circ) \sim 1.6$. This value is associated with an estimate of the transferred angular momentum $\Delta l \leq 10\hbar$. This anisotropy value has to be compared with a value of $W(0^\circ)/W(90^\circ) \sim 1.2$ measured for the same $\Delta Z = 2$ channel in this experiment. A second point of comparison is given by the data for the $^{19}\text{F} + ^{232}\text{Th}$ fusion reaction [21] that can be compared with our result for $\Delta Z = 9$ ($Z_{PLF} = 5$). In the case of $^{19}\text{F} + ^{232}\text{Th}$ reaction, typical anisotropy values are $W(0^\circ)/W(90^\circ) = 2.1-2.2$, corresponding to average angular momenta of about $35\hbar$. Our value in Fig. 7 corresponding to $\Delta Z = 9$ ($Z_{PLF} = 5$) is $W(0^\circ)/W(90^\circ) \sim 1.9$ which is close to the fusion-fission case.

To deduce the TLF angular momentum, calculations of the fission anisotropy were performed with the GANES code [22], which simulates the fission of the recoiling TLF at different angular momentum values taking into account the geometry of our apparatus. This latter point is thought to be important, due to the large angle acceptance of the BALL detectors. A comparison between calculations and experimental data indicates an increase of the TLF angular momentum, in the region of the quasielastic reaction, from $6\hbar$ at

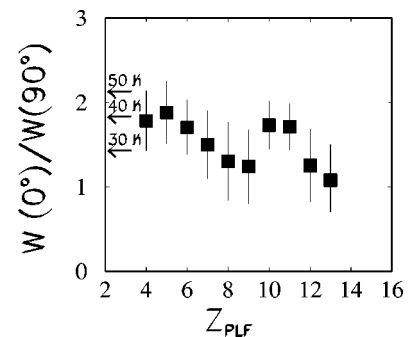


FIG. 7. Measured in-plane fission fragment anisotropies $W(0^\circ)/W(90^\circ)$ as a function of Z_{PLF} . Arrows refer to GANES calculations for fixed value of the TLF angular momentum. For details see the text.

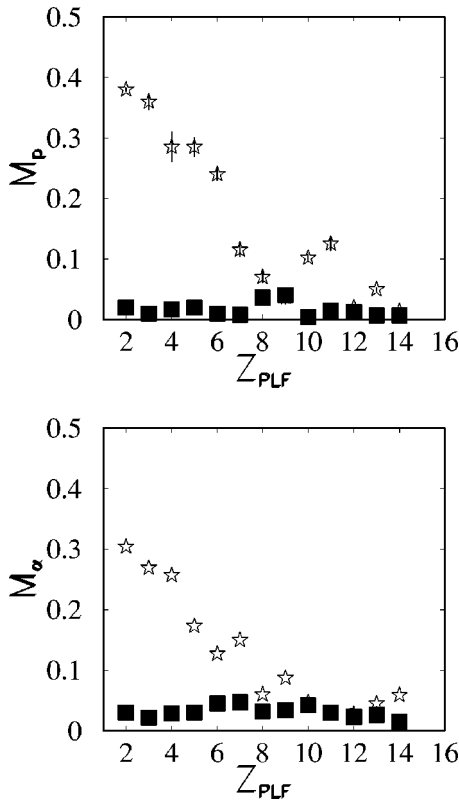


FIG. 8. Multiplicity of protons (upper panel) and alpha particles (lower panel) emitted in coincidence with projectilelike fragments of different Z_{PLF} (open stars). Data for the transfer fission channels are also reported (solid squares).

$Z_{PLF} = 13$ up to a maximum $39\hbar$ at $Z_{PLF} = 10$. This trend is consistent, as expected, to the increase of the average energy loss. For higher Z transfers, the angular momentum then features an apparent drop to $25\hbar$ at $Z_{PLF} = 9$ and then rises again in the region of deep-inelastic products, saturating at values around $40\hbar$. The discontinuity of the measured anisotropy, which is reflected in the drop of the derived angular momentum, seems to be correlated with the transition of the reaction mechanism from the quasielastic to the deep-inelastic regimes. We note that the above estimates of the angular momentum transferred to the TLF fragments are in agreement with the findings of previous works in this field [8,19]. The angular momentum values determined in this way together with the average excitation energy values from Fig. 5 have been used to fully characterize the TLF produced in the $^{28}\text{Si} + ^{232}\text{Th}$ reaction.

2. Light charged particle emission

The coincidences between projectilelike fragments and protons or alphas [indicated in the following as light charged particles (LCP's)] detected in the 8π LP spectrometer have also been studied. Results are reported in Fig. 8 in terms of the measured LCP multiplicity for proton and alpha particles as a function of Z_{PLF} , for twofold PLF-LCP events as well as for threefold PLF-LCP-fission coincidence events. As expected, an increase of the particle multiplicities is evidenced in increasing the net charge transfer. Moreover, it is observed

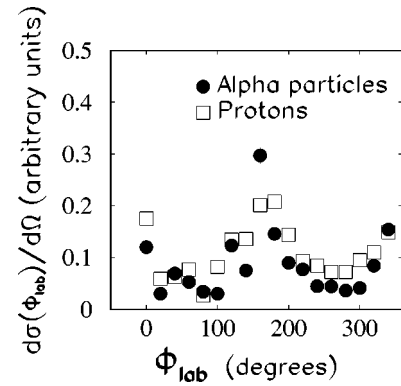


FIG. 9. Out-of-plane angular distribution of LCP's in coincidence with PLF's. For details see the text.

that for small charge transfer channels ($\Delta Z = 0-4$), the multiplicity of the alpha particles is very low and does not change significantly when a further coincidence with fission fragments is required. For larger charge transfers, the inclusive proton and alpha particle multiplicities are, on the average, about a factor of 5 larger than the ones measured in coincidence with fission fragments. This difference can be assumed to be mainly due to the particle decay from the excited TLF fragment without fission taking place at any stage of its deexcitation, over and above the emission from PLF's, which is present in both kind of events.

To better qualify the particle emission characteristics, the angular distribution of LCP's in coincidence with PLF's has been derived, as shown in Figs. 9 and 10. The out-of-plane angular distribution of PLF's with respect to the reaction plane defined by the detected PLF's and the beam axis, reported in Fig. 9, is dominated by a pronounced peak centered in the reaction plane on the opposite side of the PLF trigger ($\Phi_{lab} = 180^\circ$). This peak demonstrates that a sizable part of the LCP yield is coming from the decay of the complementary TLF's. A second, weaker component is located also in plane, from the same side of the trigger, at $\Phi_{lab} = 0^\circ$ and $\Phi_{lab} = 360^\circ$. This component is certainly associated with the PLF decay. The in-plane angular distribution, reported in Fig. 10, is obtained by considering detectors located in the reaction plane from both sides of the beam direction. It shows evidence for a relevant forward emission, at $|\Theta_{lab}| < 60^\circ$, in the angular re-

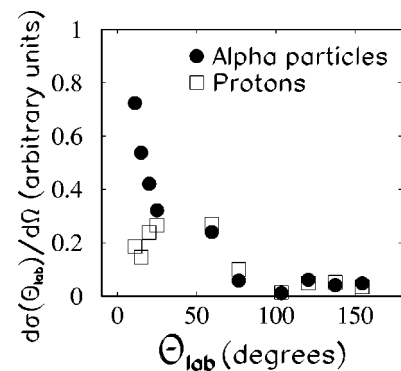


FIG. 10. In-plane angular distribution of LCP's in coincidence with PLF's. For details see the text.

gion where both the trigger PLF and the recoiling TLF are located. It is worth mentioning that this distribution looks substantially different for protons and alpha particles. The proton correlation features, indeed, a peak centered in the region of the recoiling TLF nuclei, whereas the alpha particles show a continuous increase of the yield in decreasing the observation angle.

Consequently, it appears that at least a part of the LCP emission is consistent with the assumption of a sequential decay of the fragments produced in the two-body collisions. However, the forward angular distribution of the alpha particles and the partial coverage at small angles in the present setup make impossible to disentangle a prompt emission of charged particles during the initial stage of the collision, as in case of projectile breakup [23], which is normally focused at small angles. Because of this uncertainty, the measured total charge carried away by the emitted light particles (ΔZ_{LCP}) that can be derived from the data in Fig. 8 has to be considered only as a lower limit. In any case, the values of ΔZ_{LCP} measured in coincidence with fission events are negligible, being $\Delta Z_{LCP} < 0.2$ in the limit of $Z_{PLF} > 8$. This supports the use of a simple charge conservation ($Z_{TLF} = 104 - Z_{PLF}$) in evaluating the TLF atomic number in these cases. For larger ΔZ transfer channels, the charge deficit ΔZ_{LCP} increases up to values $\Delta Z_{LCP} \approx 1$. In the latter case, more precise and detailed information on the different components contributing to the missing charge seems to be necessary to derive a reliable estimate of the TLF atomic number, especially in view of the observed enhancement of the $Z_{PLF} = 6$ evidenced in Fig. 3. We note that the LCP yield was high at the higher beam energy as reported by Eckart *et al.* [8] for 30A MeV ^{40}Ar -induced transfer fission on ^{232}Th . Therefore in their work LCP emission yields were important.

To shed more light on the LCP emission, we have performed statistical model calculations, using the PACE2 code [24]. In the model, we have artificially increased the fission barriers to hinder the fission process and force the calculations to consider only the particle decay from highly fissile nuclei at large excitation energy and angular momentum values. We have verified that in the statistical model the alpha particle emission starts to be important only for angular momentum values $J > 40\hbar$. From a quantitative point of view, the average alpha particle multiplicity values obtained from such calculations are of the same order of magnitude as the ones obtained in the experiment. It is interesting to note that the limit on the angular momentum derived in this way is in agreement with that derived from the analysis of the fission fragment angular distributions.

3. Transfer-fission yield

The ratio of fission yield to PLF singles yield Y_f has been determined by integrating the measured angular distribution of fission fragments with respect to the recoiling TLF, described in Sec. III B 1. The observed Y_f values as a function of the projectile charge Z_{PLF} are reported in Fig. 11. It is seen that Y_f first increases with increasing net charge transfer up to $\Delta Z = 4$ and then shows a plateau around the values $Y_f = 0.4 - 0.6$ followed by a decrease for the higher Z transfers. The initial rise of the fission yield is qualitatively ex-

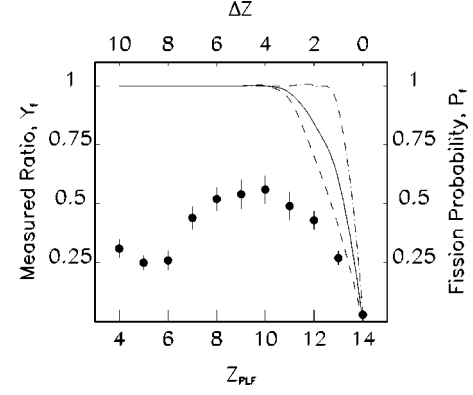


FIG. 11. Measured ratio of transfer-fission yield to PLF singles, Y_f , versus the projectile Z_{PLF} (solid squares). The net charge transfer ΔZ is also indicated. The values of fission probability P_f are calculated with the statistical model code PACE2 for the fission probability using $a_f = a_n = A/12 \text{ MeV}^{-1}$ are also shown in the figure, where solid lines correspond to the average values of the TLF parameters and the dashed and dotted lines give the limits corresponding to the estimated spread in these parameters.

pected, due to the significant increase of the average TLF angular momentum and excitation energy as well as to the decrease of fission barriers, with increasing ΔZ .

The significant survival of TLF against fission as shown in Fig. 11 can be experimentally verified for small values of ΔZ by searching for heavy, low-energy residues detected in coincidence with PLF's. While there is a reduced coverage of the BALL detectors for this specific reaction channel, TLF nuclei could still be directly detected in case of $Z_{PLF} = 11 - 14$ fragments. For these fragments the average recoil angle for the correlated TLF is within the angular acceptance of the BALL detectors although the kinematical correlation is expected to be severely spread out by the multiple scattering effects. The observation of heavy, low-energy TLF nuclei, in coincidence with $Z_{PLF} = 12$, is shown in the identification matrix reported in Fig. 12. The events corresponding to very low energy (about 5 MeV) refer to the TLF residue nuclei and these are well separated from fission fragments and light charged particles. The measured kinetic energy is

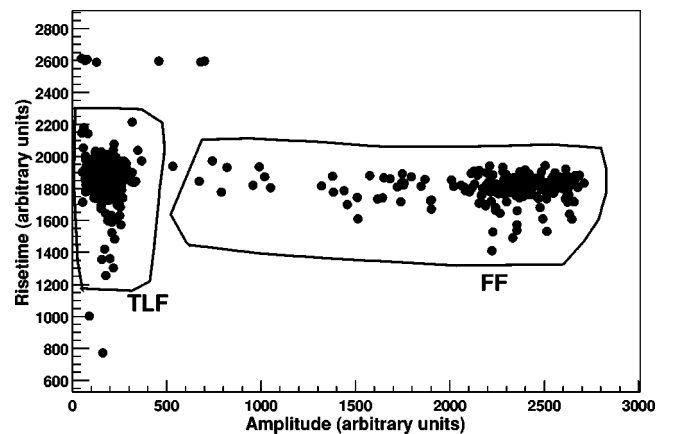


FIG. 12. Identification of TLF events in the BALL detector in coincidence with the PLF trigger $Z_{PLF} = 12$.

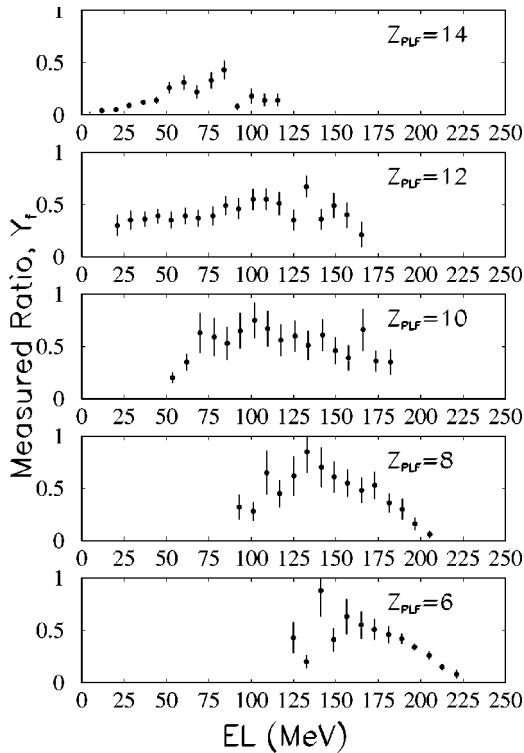


FIG. 13. Measured ratio of transfer-fission yield to PLF singles Y_f as a function of the energy loss for different projectile Z_{PLF} .

compatible with that estimated from kinematics corrected for energy loss in the target and the pulse height defect in the Si detector.

To look further in details, the observed values of Y_f for some selected Z_{PLF} are shown in Fig. 13 as a function of the measured energy loss (EL). As a general behavior, the measured Y_f first increases with EL, then shows a saturation or, in several cases, it shows a decrease for higher EL. This decrease is particularly strong in the cases of $Z_{PLF}=8$ and 6. This apparent decrease of the Y_f at higher EL goes against expectations based on the mechanism of sequential fission of TLF following a two-body collision, since the observed Y_f correspond to the cumulative fission yield distribution taking into account multiple chance fission. Thus the observed decrease of Y_f with increasing EL further supports that the reaction mechanism is more complex in the case of $\Delta Z > 6$ and high-energy losses. This is certainly to be expected not only due to more complex entrance channel reaction mechanisms such as projectile breakup but also because of sizable sequential charged particle decay.

IV. DISCUSSION

The experimental results reported above suggest that the reconstruction of the atomic number, excitation energy, and angular momentum of the undetected targetlike fissioning nucleus can be reliably achieved only in the case of small charge transfers, i.e., $\Delta Z \leq 6$. On the contrary, in case of the $\Delta Z > 6$ channels, the reaction mechanism might be more complex than a simple two-body mechanism, making difficult to reconstruct the TLF parameters. Consequently, we

confine ourselves to the $\Delta Z \leq 6$ channels in our discussion of the observed transfer-induced fission yields. It is clear that only if the first step of the reaction is characterized by a two-body reaction mechanism, the observed Y_f correspond to the fission probability P_f and therefore can be compared with the model estimates of P_f .

Under the assumption of $Y_f = P_f$ for $\Delta Z \leq 6$, the results reported in Fig. 11 show that the observed average fission probability for nuclei having atomic number $Z_{TLF} \approx 92-96$ is $P_f = 0.4-0.6$. In an earlier work [25], it has been reported that in deep-inelastic channels of the reaction 618 MeV $^{86}\text{Kr} + ^{197}\text{Au}$, P_f is close to 100% for $Z_{TLF} \approx 88-89$ nuclei. Since the values of P_f reported in Ref. [25] were found to be much larger than those obtained in the reaction 130 MeV $^4\text{He} + ^{197}\text{Au}$ [26], the enhancement of the fission probability was considered due to the higher angular momentum transferred to TLF in deep-inelastic collisions using heavy projectiles. But it was pointed out that the absolute value of the measured P_f could not be explained simply by the angular-momentum-induced effects. A more direct mechanism was proposed, leading to fission in deep-inelastic collision when the heavy fragment is stretched near or beyond the saddle point by long-range Coulomb force. Such nonequilibrium fission effects have also been reported for the reactions 12.4 MeV/nucleon ^{84}Kr on ^{90}Zr and ^{166}Er and 12.5 MeV/nucleon ^{129}Xe on ^{122}Sn [27]. Therefore, although our present results may appear in disagreement with those of Ref. [25], this may be also due to the presence of nonequilibrium fission paths in the reactions induced by Kr projectiles.

For the sake of comparison with the observed values of P_f for $\Delta Z \leq 6$, fission probabilities were calculated by using the statistical model code PACE2 with the level density parameter $a_n = a_f = A/12 \text{ MeV}^{-1}$. In these calculations, the average values of P_f were calculated for each Z_{PLF} , taking into account the spread in the excitation energy of TLF nuclei, caused by the observed spread in the EL distribution. These calculated average values of P_f are shown as solid line in Fig. 11. The limits on the average values of P_f due to the spread in the TLF parameters were also calculated and are shown by the dashed and dotted lines. The calculations predict a rapid rise of P_f with net charge transfer ΔZ , being close to the limiting value $P_f = 1$ for values of $\Delta Z \geq 3$. It may be pointed out that the use of a larger value of the level density parameter (e.g., $a_n = A/8, A/10 \text{ MeV}^{-1}$) and/or $a_f/a_n > 1$ only results in a higher values of P_f than shown in the figure. These results show that the statistical model predictions are severely overestimating the fission probabilities under all assumptions. In other words, TLF nuclei with atomic number $Z = 90-96$ populated in the transfer reactions exhibit substantially reduced fission probabilities as compared to the statistical model estimates. Consequently, the comparison suggests the presence of a significant dynamical hindrance to fission.

Furthermore, measured P_f data are compared in Fig. 14 with earlier results from Gavron *et al.* [28] for nuclei at lower excitation energies. All the nuclei studied in that work exhibit a steep rise of P_f at the fission barrier, followed by a slight decrease, due to the neutron competition in the second-chance fission. The results of Gavron *et al.* [28] together

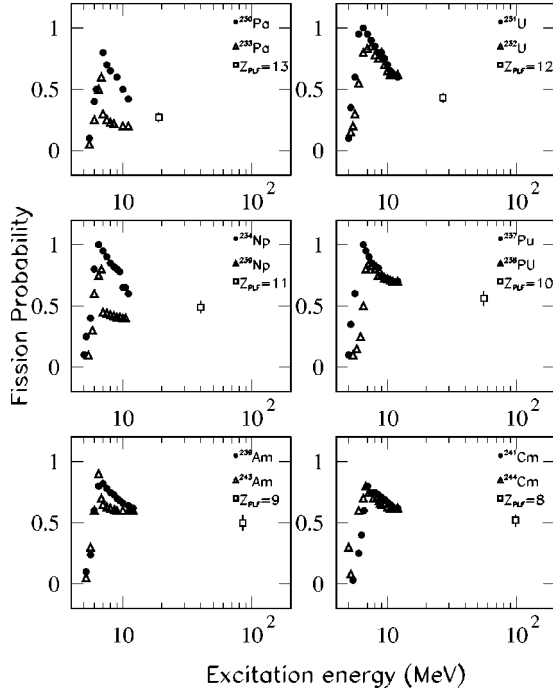


FIG. 14. Fission probability as a function of excitation energy for various TLF. Open squares are results from this work, solid circles and open triangles are results taken from Ref. [28]. For details see the text.

with our experimental findings indicate that there is not much increase in the P_f value for all systems above 20–30 MeV of excitation energy. The saturation of the fission probability at higher excitation energies means that the fission width at these higher excitation is much smaller as compared to the neutron width. As this feature cannot be understood on the basis of the statistical model, such a behavior is considered to be a consequence of a large dynamical hindrance to fission due to viscosity effects [3]. To have a more quantitative understanding, the calculated neutron lifetimes are reported in Fig. 15 as a function of the excitation energy of TLF nuclei having different atomic number. It appears from Fig. 15 that these heavy nuclei will predominantly decay by neutron emission, without any significant fission, at excitation energies above 30–50 MeV, if fission dynamical times

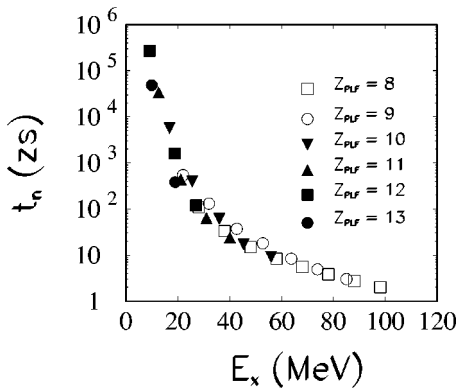


FIG. 15. Calculated neutron emission lifetimes versus excitation energy of targetlike nuclei for $a_n = A/12 \text{ MeV}^{-1}$.

are assumed to be of the order of 10–100 zs. Such larger fission dynamical times are also indicated by the measured prefission neutron multiplicities [29]. Consequently, the measured fission probabilities at higher energies correspond to the cumulative fission probabilities for the last few stages of deexcitation only, thus explaining the trend of P_f observed in our data.

The suppression of the fission probability at high excitation energies has been reported also in earlier studies, including transfer-fission channels [8,9]. In particular, Eckart *et al.* [8] have shown that sequential fission of the excited-targetlike fragments in the $^{40}\text{Ar} + ^{232}\text{Th}$ reaction is significantly hindered even at the excitation energy of 50–75 MeV. In this case, P_f values were found indeed to be in the range of $P_f = 0.4\text{--}0.7$ for $Z \approx 89$, which is consistent with the present observations. In a recent systematic study of pre- and post-scission neutron emission [7] also, it has been found that the data are consistent with the assumption that contributions to fission essentially come from the later stages of deexcitation. Furthermore, shell effects were recently observed in the fission fragment mass distributions in a study of the $^{238}\text{U} + ^{40}\text{Ar}$ reaction [30]. This was also explained by assuming that the fission does not contribute much at the initial excitation energy of the compound nucleus but only after the neutron emission. The fissioning nuclei are therefore generally cold enough to be influenced by the shell effects.

V. SUMMARY AND CONCLUSIONS

In the present work, the multinucleon transfer-induced fission reactions induced by 340 MeV ^{28}Si on a ^{232}Th target have been studied by using a large-area detection system for fission fragments and light charged particles. The projectile-like fragments, detected close to the grazing angle, show the expected transition from quasielastic reaction to the deep-inelastic reaction regime with increasing net charge transfer ΔZ . The estimated excitation energy and angular momentum transferred to the targetlike fragments also increase with increasing ΔZ and the inelasticity of the reaction.

The analysis of the light charged particles emitted in coincidence with PLF's demonstrates that only those events which do not result in TLF fission give rise to a sizable light charged particle emission. It is inferred that one can reliably reconstruct the charge, excitation energy, and angular momentum of the fissioning targetlike nucleus for the transfer channels up to $\Delta Z \leq 6$. For the corresponding TLF nuclei, statistical model calculations predict a very high fission probability ($P_f \sim 1$), at the excitation energies and spin values populated in these reactions. On the contrary, the measured ratio between transfer-fission and PLF singles Y_f , which can be identified as the fission probability P_f in the case of $\Delta Z \leq 6$, remains in the range $Y_f = 0.4\text{--}0.6$, implying that there is a sizable survival probability of TLF nuclei against fission. It may be stressed that because of the low fission barriers of the populated targetlike nuclei, model predictions are quite insensitive to the excitation energy and the angular momentum assumed to be transferred to TLF's in the collisions. The measured fission probabilities for $\Delta Z \leq 6$ can be explained only by invoking large fission dynamical times

of about 10–100 zs. Indications of such large dynamical times have been also obtained by the pre-scission neutron multiplicity measurements in this mass region. Consequently, the results reported in this work have shown that in the case of TLF's with $Z=90\text{--}96$, although the composite system was populated at high excitation energies, the fission mostly takes place from a rather cold nucleus after a substantial neutron emission in the initial stages of the deexcitation chain.

It is worth mentioning that multinucleon transfer reactions at energies close to the reaction barrier have been already used for nuclear spectroscopy studies in the Rn, Ra, and Th regions [2]. Such reactions were also indicated in the past as a useful tool to produce superheavy elements [31]. The results reported herein show that in the excited actinide nuclei there is not much significant competition from fission in spite

of low fission barriers and high excitation energies. It would therefore be of interest, from the point of view of maximizing the cross sections for the synthesis of heavy and superheavy nuclei, to consider the use of neutron-rich radioactive beams at above-barrier energies on actinide nuclei since the fused system is expected to preferentially cool down by neutron evaporation and rather than by fission in the initial stages.

ACKNOWLEDGMENTS

Thanks are due to the Laboratori Nazionali di Legnaro for providing excellent beams. A.S. and D.C.B. thank INFN for supporting their stay in Italy during the experiment. Technical support from A. Boiano (Napoli) and M. Caldogno (Padova) during the experiment is gratefully acknowledged.

-
- [1] J.B. Natowitz, M. Gonin, M. Gui, K. Hagel, Y. Lou, D. Utlej, and R. Wada, *Phys. Lett. B* **247**, 242 (1990).
 - [2] J.F.C. Cooks *et al.*, *J. Phys. G* **26**, 23 (2000), and references therein.
 - [3] D. Hilscher and H. Rossner, *Ann. Phys. (Paris)* **17**, 471 (1992).
 - [4] J. Lestone, *Phys. Rev. Lett.* **70**, 2245 (1993).
 - [5] A. Saxena, A. Chatterjee, R.K. Choudhury, S.S. Kapoor, and D.M. Nadkarni, *Phys. Rev. C* **49**, 932 (1994).
 - [6] A. Chatterjee, A. Navin, S. Kailas, P. Singh, D.C. Biswas, A. Karnik, and S.S. Kapoor, *Phys. Rev. C* **52**, 3167 (1995).
 - [7] G. Rudolf and A. Kelic, *Nucl. Phys.* **A679**, 251 (2001).
 - [8] E.M. Eckart *et al.*, *Phys. Rev. Lett.* **64**, 2483 (1990), and references therein.
 - [9] B. Djerroud *et al.*, *Phys. Rev. C* **64**, 034603 (2001).
 - [10] E. Geraci *et al.*, *Phys. Rev. C* **64**, 034609 (2001).
 - [11] Y. Aritomo, T. Wada, M. Ohta, and Y. Abe, *Phys. Rev. C* **59**, 796 (1999).
 - [12] G. Prete *et al.*, *Nucl. Instrum. Methods Phys. Res. A* **422**, 263 (1999).
 - [13] G. Pausch, M. Moszynski, D. Wolski, W. Bohne, H. Grawe, D. Hilscher, R. Schubert, G. de Angelis, and M. de Poli, *Nucl. Instrum. Methods Phys. Res. A* **365**, 176 (1995).
 - [14] National Instrument Software web address: <http://www.natinst.com>
 - [15] A. Ordine, A. Boiano, E. Vardaci, A. Zaghi, and A. Brondi, *IEEE Trans. Nucl. Sci.* **45**, 873 (1998).
 - [16] ROOT package, see <http://root.cern.ch/>
 - [17] W.U. Schroeder and J.R. Huizenga, in *Treatise on Heavy-Ion Science*, edited by D.A. Bromley (Plenum, New York, 1984), Vol. 2, p. 115, and references therein.
 - [18] R. Vandenbosch, A. Lazzarini, D. Leach, D.K. Lock, A. Ray, and A. Seamster, *Phys. Rev. Lett.* **52**, 1964 (1984).
 - [19] M. Ragjagopalan, L. Kowalski, D. Logan, M. Kaplan, J.M. Alexander, M.S. Zisman, and J.M. Miller, *Phys. Rev. C* **19**, 54 (1979).
 - [20] J.P. Lestone, J.R. Leigh, J.O. Newton, and J.X. Wei, *Nucl. Phys.* **A509**, 178 (1990).
 - [21] N. Majumdar, P. Bhattacharya, D.C. Biswas, R.K. Choudhury, D.M. Nadkarni, and A. Saxena, *Phys. Rev. C* **51**, 3109 (1995), and references therein.
 - [22] N.N. Ajitanand, G. La Rana, R. Lacey, D.J. Moses, L.C. Vaz, G.F. Peaslee, D.M. de Castro Rizzo, M. Kaplan, and J.M. Alexander, *Phys. Rev. C* **34**, 877 (1986).
 - [23] M. Samri *et al.*, *Nucl. Phys.* **A609**, 108 (1996), and references therein.
 - [24] A. Gavron, *Phys. Rev. C* **21**, 230 (1980).
 - [25] G.J. Wozniak, R.P. Schmitt, P. Glassel, R.C. Jared, G. Bizard, and L.G. Moretto, *Phys. Rev. Lett.* **40**, 1436 (1978).
 - [26] L.G. Moretto, *Physics and Chemistry of Fission, 1973* (IAEA, Vienna, 1974), Vol. 1, p. 329.
 - [27] D.V. Harrach, P. Glassel, L. Grodzins, S.S. Kapoor, and H.J. Specht, *Phys. Rev. Lett.* **48**, 1093 (1982).
 - [28] A. Gavron, H.C. Britt, E. Konecny, J. Weber, and J.B. Wilhelmy, *Phys. Rev. C* **13**, 2374 (1976).
 - [29] K. Siwek-Wilczynska, J. Wilczynski, R.H. Siemssen, and H.W. Wilschut, *Phys. Rev. C* **51**, 2054 (1995), and references therein.
 - [30] Yu. Pyatkov *et al.*, *Eur. Phys. J. A* **10**, 171 (2001).
 - [31] W. Von Oertzen, *Z. Phys. A* **342**, 177 (1992).